Geometry dependence of coercivity in Ni nanowire arrays

2008 Nanotechnology 19 075713

(http://iopscience.iop.org/0957-4484/19/7/075713)

Nanotechnology **19** (2008) 075713 (6pp) doi:10.1088/0957-4484/19/7/075713

Geometry dependence of coercivity in Ni nanowire arrays

J Escrig[1], R Lavín[1], J L Palma[1], J C Denardin[1], D Altbir[1], A Cortés[2] and H Gómez[2]

[1] Departamento de Física, Universidad de Santiago de Chile, USACH, Avenida Ecuador 3493, 917-0124 Santiago, Chile
[2] Instituto de Química, Facultad de Ciencias, Universidad Católica de Valparaíso, Casilla 4059, Valparaíso, Chile

E-mail: jescrig@usach.cl

Received 6 November 2007, in final form 12 December 2007
Published 31 January 2008
Online at stacks.iop.org/Nano/19/075713

Abstract
Magnetic properties of arrays of nanowires produced inside the pores of anodic alumina membranes have been studied by means of vibrating sample magnetometer techniques. In these systems the length of the wires strongly influences the coercivity of the array. A simple model for the coercivity as a function of the geometry is presented which exhibits good agreement with experimental results. Magnetostatic interactions between the wires are responsible for a decrease of the coercive field.

(Some figures in this article are in colour only in the electronic version)

1. Introduction

During recent years magnetic nanoparticles have attracted increasing interest due to their promising applications in hard disk drives, magnetic random access memory and other spintronic devices [1–4]. Also, these elements are good candidates for biomedical applications. The use of these particles in devices and architectures is conditioned on the possibility of having a fine control of their size and shape, keeping thermal and chemical stability of the nanoparticles [5]. For such applications, different geometries have been considered [6–10]. In particular, highly ordered arrays of magnetic nanowires produced inside the pores of anodic alumina membranes by electrochemical deposition [11] have been the focus of intense research [12–15]. The high ordering, together with the magnetic nature of the wires, gives rise to outstanding cooperative properties different from the bulk and even from film systems. In these arrays, inter-element interactions play an important role and have been the subject of strong investigation. Kazadi Mukenga Bantu *et al* [16] and Rivas *et al* [17] investigated the structure and magnetic properties of cobalt nanowires and observed a change of the easy axis depending on the magnetostatic interactions between them. More recently, Gubbiotti *et al* [18] and Goolaup *et al* [19] reported that the switching behaviour of the wires is affected by magnetostatic interactions. In such particles, the understanding of the magnetization reversal mechanisms is a permanent challenge for researchers. It has been reported independently by Forster *et al* [20] and Hertel [21] that soft magnetic nanowires can switch in two different modes depending on their thickness. These modes have become known as the transverse reversal mode and the vortex wall mode. The first refers to a thin ferromagnetic wire (diameter $d < 60$ nm). If a wire is thin enough, the exchange interaction forces the magnetization to be homogeneous through any radial cross section of the cylinder [22]. Similar reversal modes were found by Landeros *et al* [23] in the case of magnetic nanotubes.

For small particles, the Stoner–Wohlfarth model has been applied to calculate the coercivity when the reversal of magnetization is driven by a coherent rotation [24]. Also Aharoni [25] calculated the nucleation field in a prolate spheroid when the reversal is driven by curling rotation. However, when the transverse reversal mode appears, the coercivity has not been modelled yet. Thus, usually experimental results for the coercivity in this case are interpreted using the Stoner–Wohlfarth model [26].

In this paper we present experimental results for high aspect ratio Ni nanowire arrays. Based on micromagnetic calculations, the coercivity in the presence of a transverse reversal mode is modelled, showing good agreement with experiments. Magnetostatic interactions are included in order to investigate its effect on the magnetic properties of the array.

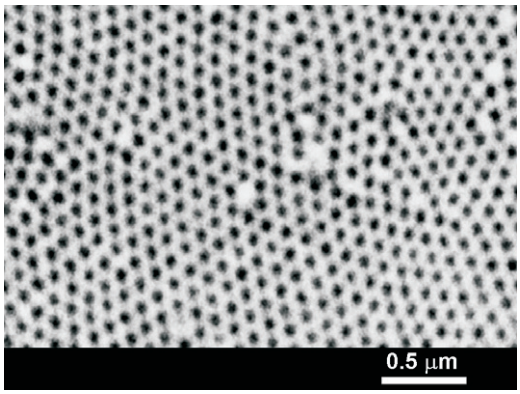

Figure 1. SEM top view of a highly ordered home-made AAO template.

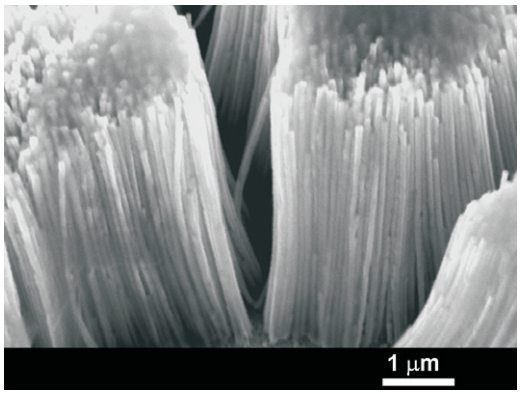

Figure 2. SEM image of the exposed Ni nanowires with diameter of 50 nm after the alumina template membrane was dissolved away. Magnification: 17 000×.

2. Experimental methods

The anodic alumina oxide (AAO) porous membranes were prepared from a 99.99% aluminium foil (0.13 mm thickness, Sigma-Aldrich) by the two-step anodization technique [27]. The grease on the aluminium surface was removed with detergent, then successively with acetone and water. The cleaned aluminium sheets were submitted to an annealing at 350 °C in air for 1 h using a Lindgerg/Blue M model tube furnace. Then, the aluminium sheets were first etched with a 5% w/w NaOH solution and afterwards with diluted nitric acid. Subsequently, the samples were mechanically polished with alumina (0.3 and 0.05 μm mesh) followed by 1 min of electropolishing at 15 V in a 40% H_2SO_4, 59% H_3PO_4, 1% glycerine bath. After this treatment the samples were submitted to a first anodization at 40 V for 6 h in a 0.3 M oxalic acid solution at 20 °C. The anodized layer was etched with a 5% H_3PO_4 and 1.8% $H_2Cr_2O_4$ solution at room temperature for 12 h. The ordered pore arrangement was achieved with a second anodization step that was performed in the same conditions as in the first one. A 0.1 M $CuCl_2$ and 20% v/v HCl solution at room temperature was employed to remove the remaining aluminium from the alumina substrate. To remove the barrier layer and to open the pores at the bottom, the membrane was first treated with 5% H_3PO_4 and 5% NaOH aqueous solution at room temperature. Subsequently, the pores were widened in a 0.085 M H_3PO_4 solution at 37 °C for 15 min. As is observed in figure 1, the membranes present highly ordered pores of diameter $d = 2R = 50$ nm and lattice constant $D = 100$ nm. To facilitate the electrical contact, a very thin Au–Pd layer was sputtered on one side of the membrane followed by the electrodeposition [28] of a thicker nickel layer to achieve the full pore sealing. In this paper the electrodeposition was performed at a constant potential (dc electrodeposition at −0.9 V). The potentiostatic condition allows us to have more precise control of the electrochemical reaction, and then a more accurate control of the growth of the Ni nanowires.

The morphology and the single-crystalline structure of individual nanowires were subsequently investigated by scanning electron microscopy (SEM) and transmission electron microscopy (TEM) after dissolution of the template.

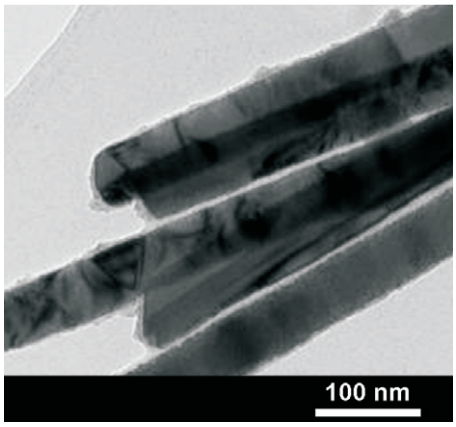

Figure 3. TEM image of free-standing Ni nanowires that have been grown at −0.9 V.

A JEOL 5900 LV apparatus was used for SEM measurements. Figure 2 shows the SEM images of nickel nanowires grown into the 50 nm home-made alumina template supported on the substrate. This figure shows that the nanowires have a high aspect ratio, are well defined, parallel and close to each other.

TEM observations were carried out on a JEOL 2010F electron microscope operated at 200 kV coupled with an energy-dispersive spectrometer Princeton Gamma Technology system. A 1 nm diameter probe was used for the microanalysis. Samples were prepared by crushing glass samples in an agate mortar and ultrasonically stirring them in butanol. The smallest particles are then collected in the supernatant liquid using a holey C-coated copper grid. Figure 3 shows a TEM image of continuous free-standing nanowires. Both analyses account for a continuous growth that follows the shape of the pores' template.

Chemical characterization of nanowires has been realized by means of energy-dispersive analysis of x-rays (EDAX). Figure 4 shows the spectroscopy data. The peaks correspond to characteristic elemental emissions of Ni.

The magnetic properties of the Ni nanowires were measured by a vibrating sample magnetometer (VSM). Figure 5 illustrates the hysteresis cycles for two samples with

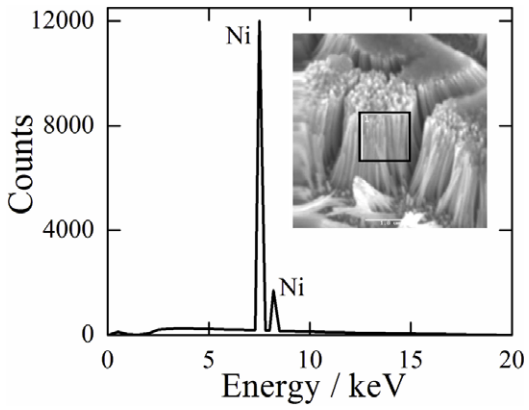

Figure 4. EDAX spectroscopy of a selected area in the Ni nanowire array. The peaks correspond to characteristic elemental emissions of nickel.

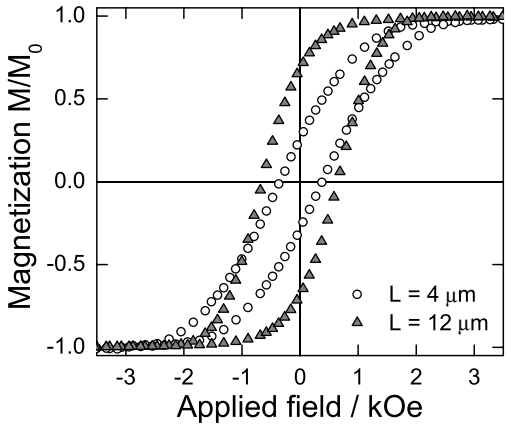

Figure 5. Hysteresis cycles for Ni nanowires (50 nm diameter and 100 nm interwire distance) as a function of the length. The magnetic field is applied parallel to the wire axis.

diameter $d = 50$ nm, lattice parameter $D = 100$ nm and lengths $L = 4$ and 12 μm, measured with the external field along the axis of the wires. From the comparison of these loops, an increase of the coercivity and the remanence in relation to the length has been observed. Therefore we observed that the magnetic behaviour of the arrays is strongly dependent on the effective magnetic anisotropy (mainly determined by shape).

3. Model and discussion

In order to investigate this behaviour, we propose a model which leads us to calculate the coercivity as a function of the geometry. We start calculating the coercive field of an isolated magnetic nanowire assuming that the magnetization reversal is driven by a transverse mode.

3.1. Isolated magnetic nanowires

For isolated magnetic Ni nanowires with diameters smaller than 60 nm, the magnetization reversal, that is, the change of the magnetization from one of its energy minima ($\mathbf{M} = M_0\hat{\mathbf{z}}$) to the other ($\mathbf{M} = -M_0\hat{\mathbf{z}}$), occurs by means of the propagation of a transverse domain wall [23]. In this case, a domain wall appears at one end of the wire and propagates towards the other. Starting from the equations presented by Landeros *et al* [23], we can calculate the width of the domain wall for the transversal reversal mode as a function of the radius, R.

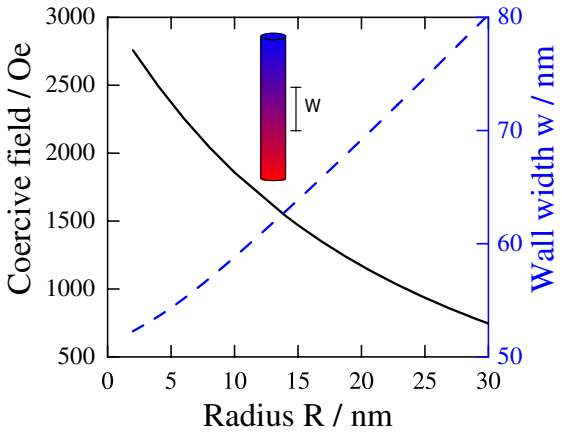

Figure 6. Coercivity (solid line, equation (1)) and wall width (dotted line) as a function of the radius of an isolated Ni nanowire. This result is independent of the length of the wire.

To calculate the coercive field of an isolated magnetic wire, H_0, we used an adapted Stoner–Wohlfarth model [24] in which the length of the coherent rotation is replaced by the width of the domain wall, w. Following this approach,

$$\frac{H_0}{M_0} = \frac{2K(w)}{\mu_0 M_0^2}, \tag{1}$$

where $K(l) = \frac{1}{4}\mu_0 M_0^2(1 - 3N_z(l))$ and $N_z(l)$ corresponds to the demagnetizing factor along z [29], given by $N_z(l) = 1 - F_{21}[\frac{4R^2}{l^2}] + \frac{8R}{3\pi l}$, where $F_{21}[x] = F_{21}[-1/2, 1/2, 2, -x]$ is a hypergeometric function.

The dependence of the coercivity H_0 (solid line) and width of the domain wall (dotted line) is depicted in figure 6 as a function of the radius of the isolated wire. In this figure we have considered Ni nanowires defined by $M_0 = 4.85 \times 10^5$ A m^{-1} and the stiffness constant $A = 10^{-11}$ J m^{-1}. In equation (1) the length involved is the width of the domain wall. However, Landeros *et al* [23] have shown that the width of the domain wall, w, is independent of the length of the wire, L, provided the wire is long enough. Then, the coercivity in figure 6 is independent of the length of the wire. However, in figure 5 we have seen a strong dependence of the coercive field on the length of the wires. Moreover, the value computed from equation (1) is greater than the experimental data. Then it is clear that the array cannot be considered simply as a set of independent wires and interactions have to be included in order to obtain a better agreement with experiments.

3.2. Array of magnetic nanowires

If each individual nanowire is treated as a non-interacting magnetic dipole, it will contribute to the whole hysteresis loop

of the array with a small square-shaped loop. Consequently, in the case of an array of identical non-interacting wires, a square macroscopic hysteresis loop would be observed with a single Barkhausen jump. Nevertheless, in the array, the distances between the wires are smaller or comparable to their diameter and/or length. Then the wires in the array are subject to important magnetostatic interactions between them that must be considered. The interaction of each wire with the stray fields produced by the array—an effective antiferromagnetic coupling between neighbouring wires—strongly influences the coercivity [30–33]. This stray field depends on the length of the wires, explaining in this way our results in figure 5. In these interacting systems, the process of magnetization reversal can be viewed as the overcoming of a single energy barrier, ΔE. In an array with all the wires initially magnetized in the same direction, the magnetostatic interaction between neighbouring wires favours the magnetization reversal of some of them. A reversing field aligned opposite to the magnetization direction lowers the energy barrier, thereby increasing the probability of switching. The dependence of the applied field on the energy barrier is often described [34] by the expression

$$\Delta E = U\left(1 - \frac{H}{H_0}\right)^2,$$

where H is the applied field and H_0 denotes the intrinsic coercivity of an isolated wire. For single-domain particles having a uniaxial shape anisotropy, the energy barrier at zero applied field, U, is just the energy required to switch by coherent rotation, $K(L)$. If we assume that the switching field H_s is equal to H_c, then

$$H_c = H_0 - H_{int}, \tag{2}$$

where H_{int} corresponds to the stray field induced within the array given by

$$H_{int} = \frac{2K(L)}{\mu_0 M_0^2}\left(\frac{\varepsilon|\tilde{E}_{int}(D)|}{K(L)}\right)^{1/2}. \tag{3}$$

In the previous equation we have assumed that the reversal of individual nanowires produces a decrease of the magnetostatic energy E_{int} that equals the magnetic anisotropy barrier ΔE. Besides, ε is an adjustable parameter that depends on the distribution of magnetic wires in space and on the long-distance correlation among the wires. The value of ε cannot be obtained from first principles, although values between unity and some tens are reasonable [35]. Besides, $\tilde{E}_{int}(D)$ is the magnetostatic interaction between two nanowires separated a distance D. Such an interaction has been calculated by Laroze *et al* [36] and is given by

$$\tilde{E}_{int}(D) \equiv \frac{E_{int}(D)}{V} = \frac{\mu_0 M_0^2 R^2}{2LD}\left(1 - \frac{1}{\sqrt{1+\frac{L^2}{D^2}}}\right).$$

In order to understand the role of the length of the wires in the array we calculate the normalized magnetostatic interaction energy per wire (no dimensional stray field) for arrays of different lengths, $\sum_{i=1}^{N-1}\sum_{j=i+1}^{N}(\tilde{E}_{int}(D)/\mu_0 M_0^2 N)$. As stated

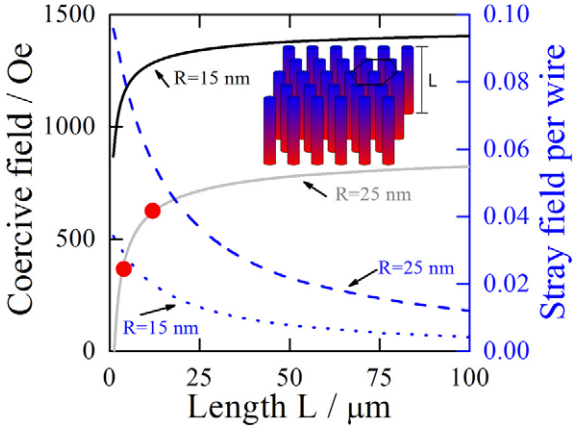

Figure 7. Calculated coercivity obtained from equation (2) using $\varepsilon = 20$ (black solid line corresponds to $R = 15$ nm and grey solid line to $R = 25$ nm) and stray fields (dotted line corresponds to $R = 15$ nm and dashed line to $R = 25$ nm) as a function of the length of the Ni nanowire arrays. Red dots correspond to the coercive fields obtained from figure 5. Interwire distance for all cases is $D = 100$ nm.

by Escrig *et al* [14], to avoid size-dependent results, we have considered a sample which contains a minimum of $N \approx 70\,000$ wires. The calculated coercivity H_c and stray field per wire as a function of the length of the wires for two different radii are depicted in figure 7, where $\varepsilon = 20$ has been used. A strong influence of the length is observed which can be ascribed to the strength of the magnetostatic interaction among nanowires, which in turn depends on the length. At small lengths an almost linear dependence of the coercivity is observed, which was previously measured by Vázquez *et al* [37]. However, in dot arrays, $d > L$, a different behaviour is observed in which case the coercivity decreases (H_{int} increases with L) [38]. In figure 7, dots illustrate the coercive fields obtained from the hysteresis loops shown in figure 5. A good agreement between the coercivities obtained with VSM and our analytical calculations is shown.

We now investigate the dependence of the coercivity on the diameter of the wires, d, and the interwire distance, D, by defining the ratio d/D. When the wires are in contact, $d/D = 1$; when they are infinitely separated, $d/D = 0$. Our results are shown in figure 8 for two different radii and four different lengths, where $\varepsilon = 20$ has been used. In the range of parameters considered, we observe that an increase of the ratio d/D results in a decrease of the coercivity. As also shown in figure 7, an increase in the length of the wires produces an increase of the coercivity.

Labelled dots 1, 2, 3 and 4 in figure 8 correspond to the cases described in table 1. Note the agreement between experimental and calculated values through equation (2). Deviations between experimental measurements and analytical results can originate from the dispersion of the lengths and positions of each wire in the array and a reduction in the homogeneity of the diameter of nanopores [37]. Also it is important to point out that in our model we have not considered any kind of crystalline anisotropy, which can be present, depending on the different synthesis procedures. The addition

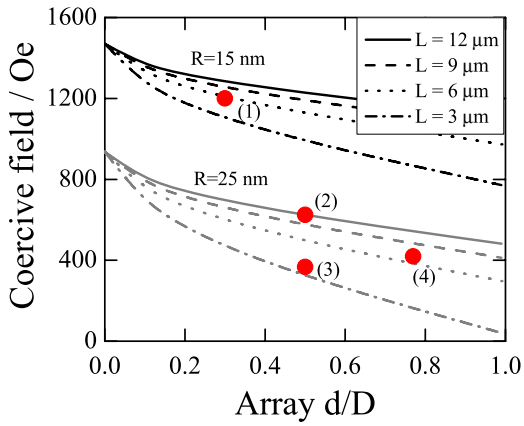

Figure 8. Dependence of calculated coercivity with the ratio of the diameter, $d = 15$ nm (black lines) and 25 nm (grey lines), to lattice parameter, D. We have used $\varepsilon = 20$. Experimental points 1, 2, 3 and 4 are discussed in the text.

Table 1. Parameters for different Ni nanowire arrays. Geometrical parameters and H_c have been measured in this paper (superscript 1) or taken from [39] (superscript 2) and [40] (superscript 3).

Dot	d (nm)	D (nm)	L (μm)	H_c (Oe)
$1^{(2)}$	30	100	$\approx$1	1200
$2^{(1)}$	50	100	$\approx$12	624
$3^{(1)}$	50	100	$\approx$4	366
$4^{(3)}$	50	65	$\approx$3	420

of such anisotropy does not modify qualitatively the results, and its effect is equivalent to changing the aspect ratio of the wire.

4. Conclusions

In conclusion, by means of analytical calculations and experimental measurements we have investigated the important role of magnetostatic interaction in the magnetic properties of nanowire arrays. We have derived an analytical expression that allows us to obtain the coercivity as a function of the magnetostatic interactions present in the array. The effect of the stray field originating from the magnetostatic interactions between the wires of the array must be included to obtain a quantitative agreement between experimental and theoretical results. Our results lead us to conclude that the length of the wires strongly influences the coercivity of the array. Good agreement between VSM measurements and theoretical calculations is obtained.

Acknowledgments

This work was supported by the Millennium Science Nucleus *Basic and Applied Magnetism* P06-022F, Fondecyt no. 11070010 and AFOSR no. FA9550-07-1-0040. The CONICYT PhD program and Graduate Direction of Universidad de Santiago de Chile are also acknowledged.

References

[1] Koch R H, Deak J G, Abraham D W, Trouilloud P L, Altman R A, Lu Yu, Gallagher W J, Scheuerlein R E, Roche K P and Parkin S S P 1998 *Phys. Rev. Lett.* **81** 4512–5
[2] Cowburn R P, Koltsov D K, Adeyeye A O, Welland M E and Tricker D M 1999 *Phys. Rev. Lett.* **83** 1042–5
[3] Wolf S A, Awschalom D D, Buhrman R A, Daughton J M, von Molnar S, Roukes M L, Chtchelkanova A Y and Treger M 2001 *Science* **294** 1488–95
[4] Gerrits Th, van der Berg H A M, Hohlfeld J, Bar L and Rasing Th 2002 *Nature* **418** 509–12
[5] Puntes V F, Krishnan K M and Alivisatos A P 2001 *Science* **291** 2115
[6] Landeros P, Escrig J, Altbir D, Laroze D, d'Albuquerque e Castro J and Vargas P 2005 *Phys. Rev.* B **71** 094435
[7] Wachowiak A, Wiebe J, Bode M, Pietzsch O, Morgenstern M and Wiesendanger R 2002 *Science* **298** 577–580
[8] Landeros P, Escrig J, Altbir D, Bahiana M and d'Albuquerque e Castro J 2006 *J. Appl. Phys.* **100** 044311
[9] Bachmann J, Jing J, Knez M, Barth S, Shen H, Mathur S, Gosele U and Nielsch K 2007 *J. Am. Chem. Soc.* **129** 9554–5
[10] Escrig J, Altbir D and Nielsch K 2007 *Nanotechnology* **18** 225704
[11] Masuda H and Fukuda K 1995 *Science* **268** 1466
[12] Nielsch K, Wehrspohn R B, Barthel J, Kirschner J, Gosele U, Fischer S F and Kronmuller H 2001 *Appl. Phys. Lett.* **79** 1360
[13] Wang Z K, Lim H S, Zhang V L, Goh J L, Ng S C, Kuok M H, Su H L and Tang S L 2006 *Nano Lett.* **6** 1083–6
[14] Escrig J, Altbir D, Jaafar M, Navas D, Asenjo A and Vázquez M 2007 *Phys. Rev.* B **75** 184429
[15] Liu M, Lagdani J, Imrane H, Pettiford C, Lou J, Yoon S, Harris V G, Vittoria C and Sun N X 2007 *Appl. Phys. Lett.* **90** 103105
[16] Kazadi Mukenga Bantu A, Rivas J, Zaragoza G, Lopez-Quintela M A and Blanco M C 2001 *J. Appl. Phys.* **89** 3393
[17] Rivas J, Kazadi Mukenga Bantu A, Zaragoza G, Blanco M C and Lopez-Quintela M A 2002 *J. Magn. Magn. Mater.* **249** 220–7
[18] Gubbiotti G, Tacchi S, Carlotti G, Vavassori P, Singh N, Goolaup S, Adeyeye A O, Stashkevich A and Kostylev M 2005 *Phys. Rev.* B **72** 224413
[19] Goolaup S, Adeyeye A O and Singh N 2006 *J. Appl. Phys.* **100** 114301
[20] Forster H, Schrefl T, Scholz W, Suess D, Tsiantos V and Fidler J 2002 *J. Magn. Magn. Mater.* **249** 181
[21] Hertel R 2002 *J. Magn. Magn. Mater.* **249** 251
[22] Hertel Riccardo and Kirschner Jurgen 2004 *Physica* B **343** 206–10
[23] Landeros P, Allende S, Escrig J, Salcedo E, Altbir D and Vogel E E 2007 *Appl. Phys. Lett.* **90** 102501
[24] Stoner E C and Wohlfarth E P 1948 *Phil. Trans. R. Soc.* A **240** 599
Stoner E C and Wohlfarth E P 1991 *IEEE Trans. Magn.* **27** 3475 (Reprinted)
[25] Aharoni A 1997 *J. Appl. Phys.* **82** 1281
[26] Wegrowe J-E, Kelly D, Franck A, Gilbert S E and Ansermet J-Ph 1999 *Phys. Rev. Lett.* **82** 3681
[27] da Fontoura Costa L, Riveros G, Gómez H, Cortés A, Gilles M, Dalchiele E A and Marotti R E 2005 http://arxiv.org/cond-mat/0504573
[28] Cortés A, Palma J L, Denardin J C, Marotti R E, Dalchiele E A and Gomez H 2007 unpublished

[29] Beleggia M, Tandon S, Zhu Y and De Graef M 2004 *J. Magn. Magn. Mater.* **272–276** e1197
[30] Adeyeye A O, Bland J A C, Daboo C and Hasko D G 1997 *Phys. Rev.* B **56** 3265
[31] Hertel R 2001 *J. Appl. Phys.* **90** 5752
[32] Vázquez M, Pirota K, Hernández-Vélez M, Prida V M, Navas D, Sanz R, Batallán F and Velázquez J 2004 *J. Appl. Phys.* **95** 6642
[33] Bahiana M, Amaral F S, Allende S and Altbir D 2006 *Phys. Rev.* B **74** 174412
[34] Sharrock M P 1994 *J. Appl. Phys.* **76** 6413–8
[35] Allia P, Coisson M, Tiberto P, Vinai F, Knobel M, Novak M A and Nunes W C 2001 *Phys. Rev.* B **64** 144420
[36] Laroze D, Escrig J, Landeros P, Altbir D, Vazquez M and Vargas P 2007 *Nanotechnology* **18** 415708
[37] Vázquez M, Pirota K, Torrejón J, Navas D and Hernández-Vélez M 2005 *J. Magn. Magn. Mater.* **294** 174
[38] Grimsditch M, Jaccard Y and Schuller I K 1998 *Phys. Rev.* B **58** 11539
[39] Nielsch K, Wehrspohn R B, Barthel J, Kirschner J, Fischer S F, Kronmuller H, Schweinbock T, Weiss D and Gosele U 2002 *J. Magn. Magn. Mater.* **249** 234–40
[40] Navas D 2006 *PhD Thesis* Universidad Autónoma